Side-by-side laboratory comparison of space heat extraction rates and thermal energy use for radiant and all-air systems

Jonathan Woolley[@ a,], Stefano Schiavon[a] , Fred Bauman[a], Paul Raftery[a], Jovan Pantelic[a]
[a] Center for the Built Environment, University of California Berkeley
[@]Address for correspondence:
Center for the Built Environment
University of California Berkeley
390 Wurster Hall
Berkeley, CA 94720, USA
Phone: +1 530-204-7619
Email: jmwoolley@berkeley.edu

ABSTRACT

Radiant cooling systems extract heat from buildings differently than all-air cooling systems. These differences impact the time and rate at which heat is removed from a space, as well as the total amount of thermal energy that a mechanical system must process each day. In this article we present measurements from a series of multi-day side-by-side comparisons of radiant cooling and all-air cooling in a pair of experimental testbed buildings, with equal heat gains, and maintained at equivalent comfort conditions (operative temperature). The results show that radiant cooling must remove more heat than all-air cooling – 2% more in an experiment with constant internal heat gains, and 7% more with periodic scheduled internal heat gains. Moreover, the peak sensible space heat extraction rate for radiant cooling (heat transfer at the cooled surface, not the cooling plant) must be larger than the peak sensible space heat extraction rate for all-air systems, and it must occur earlier. The daily peak sensible space heat extraction rate for the radiant system was 1–10% larger than for the all air system, and it occurred 1–2 hours earlier. These findings have consequences for the design of radiant systems. In particular, this study confirms that cooling load estimates for all-air systems will not represent the space heat extraction rates required for radiant systems.

GRAPHICAL ABSTRACT

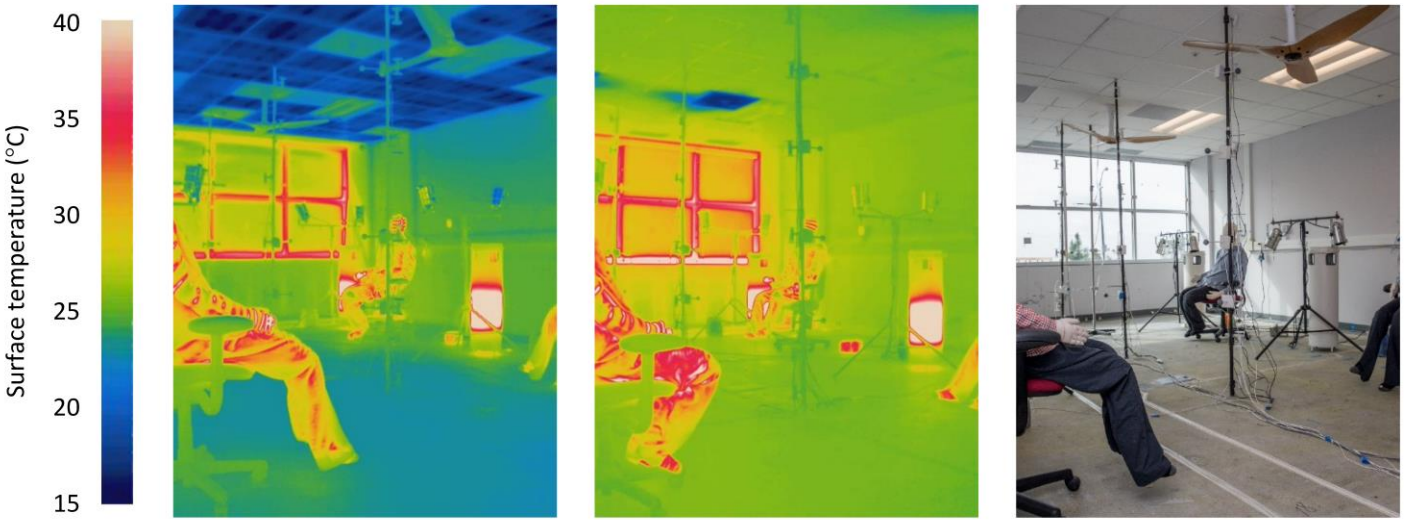

Equal comfort conditions			Environmental conditions
26 °C	Operative temperature	26 °C	Outdoor air temp. ≈ 30 °C
≈ 26.5 °C	Air temperature	≈ 25.5 °C	Exterior surface temp. ≈ 60 °C
≈ 25.5 °C	Mean radiant temp.	≈ 26.5 °C	

KEYWORDS

Radiant cooling, cooling load, energy efficiency, HVAC, laboratory experiment, all-air

HIGHLIGHTS

- Interior surface temperatures are lower in buildings with radiant cooling
- Buildings with radiant cooling store less heat in non-active masses
- Buildings with all-air cooling systems reject more heat by passive means
- Radiant cooling must remove more heat to maintain equivalent comfort conditions
- The peak sensible space heat extraction rate for radiant surfaces must be larger than for all-air system

1. INTRODUCTION

Radiant cooling and heating could be a pathway to reduce energy use and peak electrical demand in buildings compared to conventional all-air systems. A recent survey assessment of commercial building energy consumption in the United States indicated that the median energy use intensity for buildings with radiant cooling is 14–66% lower than standard buildings of comparable type and climate zone (Higgins 2017). Although radiant cooling is currently installed in a small portion of buildings overall, it is a common strategy among buildings with the lowest energy use intensity (NBI 2012, Maor 2016, Paliaga 2016). The number of high performance buildings with zero net energy aspirations has increased rapidly in recent years (NBI 2016), and consequently application of radiant cooling appears to be expanding.

Several researchers have identified reasons that radiant cooling can reduce energy consumption and peak electrical demand compared to all-air systems. We summarize the variety of explanations as five specific energy advantages for radiant cooling:

1. Electricity use for thermal distribution in radiant buildings can be lower than in all-air buildings. Airflow in radiant buildings can be limited to the minimum ventilation requirements. So, although radiant buildings require more electricity for pumping, the fan electricity savings in radiant buildings can be much larger than the increase in electricity use for pumping.
2. Radiant cooling can operate with relatively warm chilled-water temperatures. Cooling plant efficiency can be improved if chillers are designed and controlled to operate at warmer temperatures. Further, radiant cooling can also allow use of very high efficiency cooling plants, such as evaporative fluid coolers and direct ground or water body heat exchange.
3. The air temperature in buildings with radiant cooling is somewhat warmer than in buildings with all-air systems at equivalent comfort conditions. Consequently, heat gains from ventilation air are somewhat smaller for radiant and there are more hours when outdoor air provides free cooling.
4. By decoupling ventilation from space cooling, radiant systems can avoid the need for terminal reheat, and can avoid energy consumed by incidental dehumidification that occurs when air is cooled with low temperature chilled-water, or direct expansion.
5. High thermal mass radiant systems can allow for cooling plant operation during non-peak periods when electricity tariffs are lower, and when primary cooling sources may operate more efficiently.

When these advantages operate together, the potential savings for radiant cooling can be high. Numerous simulation studies and field evaluations have concluded that radiant cooling can consume much less energy than conventional all air systems.

There has been substantial research to develop and validate building energy simulation tools that properly capture the fundamental heat transfer mechanisms involved with radiant cooling systems (Strand 2002, Strand 2005, Yu 2014, Niu 1995, Niu 1997). Yet despite the variety of simulation studies that have utilized these tools to compare the primary energy performance of radiant and all-air systems, only Feng et al. and Niu et al. have explicitly compared the dynamic space heat extraction rates for radiant and all-air cooling systems (Feng 2013, Feng 2014-A, Feng 2014-B, Niu 1995, Niu 1997). Through simulation and laboratory experiments these researchers demonstrated that:

1. Radiant cooling systems extract heat from gains earlier than all-air cooling systems
2. Envelope heat transfer rates are different for radiant and all-air cooling systems
3. The daily maximum space heat extraction rate is larger for radiant cooling systems
4. The total amount of heat extracted each day is larger for radiant cooling systems

The dynamic space heat extraction rate required to maintain comfort is crucial for design, sizing, and control of any cooling system, yet as Feng et al. (2013, 2014) highlighted, industry common practice methods for design sizing of cooling systems do not properly capture the differences between radiant and all-air systems. The space heat extraction rate is the rate at which heat is removed from a space by terminal heat transfer devices. The instantaneous space heat extraction rate required to maintain comfort is not equal to the instantaneous sum of heat gains in a space because a portion of the heat gains is absorbed by non-active masses and does not immediately result in a need for active cooling. For all-air systems the space heat extraction rate is the sensible enthalpy difference between supply and return (or room air outlet) air flows. For radiant systems the space heat extraction rate is the sum of convective and radiant (longwave and shortwave) heat transfer rates at the actively cooled surface. For high thermal mass radiant systems, the space heat extraction rate will be much different from the rate at which heat is transferred to the hydronic system. Generally, design of a cooling system should begin with an assessment of the space heat extraction rates that will be required to counterbalance the effect of expected heat gains in order to achieve desired comfort conditions. When this is known, mechanical systems and controls can be designed with the ability to provide the required space heat extraction rates. Each of these heat transfer rates are defined in Figure 1.

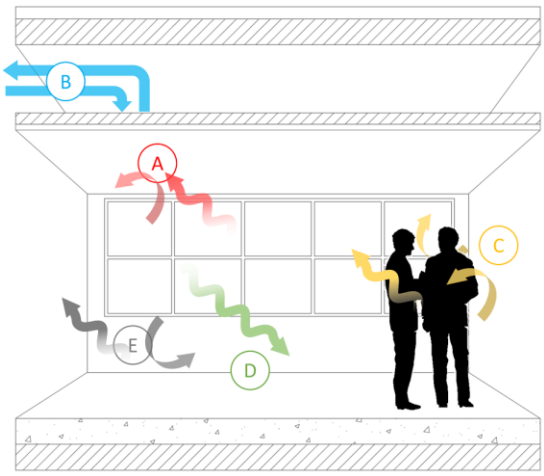

(A) **Space heat extraction rate:** the rate at which thermal energy is removed from a space by terminal heat transfer devices.

For radiant system: the sum of the convective and radiant (longwave and shortwave) heat transfer rates at the chilled surface.

For all-air system: the sensible enthalpy difference between supply and return air flow (not shown in figure).

(B) **Hydronic heat extraction rate:** the rate at which thermal energy is removed by the hydronic system, calculated as the enthalpy difference between supply and return chilled water flow.

(C) **Internal heat gain rate:** the sum of convective and radiant (longwave and shortwave) heat gain from internal sources (eg: people, lights, equipment).

(D) **Solar heat gain rate:** the rate at which electromagnetic energy from the sun is transmitted through glazing and absorbed by surfaces within the space.

(E) **Envelope heat transfer rate:** the net sum of convective and radiant heat transfer rates at the interior surface of the exterior envelope.

Figure 1: Illustration and definition of terminology used throughout this article to describe various heat transfer rates. In this article we are principally concerned with the difference between the space heat extraction rate required by radiant and all-air systems to maintain equivalent comfort conditions. In all circumstances this article is limited to sensible heat transfer only.

In this article we expand on the current understanding of radiant cooling with observations from simultaneous tests of radiant cooling and all-air cooling in side-by-side experimental testbed buildings. The specific objectives of the comparison were to observe differences in:

1. The dynamic space heat extraction rates required to maintain equivalent comfort in both testbeds
2. The cumulative amount of thermal energy extracted by each system
3. The distribution of thermal energy in masses in each testbed

To be clear, this article is principally concerned with comparing the space heat extraction rates that are required by radiant cooling and all-air cooling systems to maintain a desired operative temperature. We do not address the multitude of considerations that must be made for design of the cooling plant, thermal distribution systems, and controls which ultimately result in space heat extraction.

Only one previous laboratory study (Feng 2014) has compared the space heat extraction rates for radiant and all-air systems. That study provided clear foundational evidence about the differences between these systems, but it imposed atypical heat gains, used a relatively small adiabatic environmental chamber,

imposed somewhat inequivalent initial conditions, and only observed differences in the dynamic space heat extraction rates over a single heat gain cycle. We build on the conclusions of Feng et al. by comparing the two system types in more realistic circumstances, with various heat gain schedules, and over an extended period of time.

2. METHODOLOGY

We conducted a series of controlled experiments in a pair of equivalent testbed buildings – one with radiant cooling and one all-air cooling. The testbed buildings at Lawrence Berkeley National Laboratory FLEXLAB (FLEXLAB 2017) enable thorough assessment of building energy systems at a realistic physical scale, with naturally occurring solar gains, and natural interaction with the surrounding environment. For each experiment we operated the two testbeds simultaneously, imposed equivalent internal gains, and controlled each system to maintain equivalent operative temperatures.

In this article, we present results from two experiments, one with constant internal gains, and one with periodic internal gains. We operated each experiment for several days, during which we monitored thermodynamic states and heat transfer rates in both testbeds. It is important to compare these systems over the course of several days to ensure that the temperature of masses in each testbed reach steady-state oscillations that are no longer influenced by the initial states of each system.

For our comparison of radiant and all-air cooling we measured: air temperature distribution, operative temperature distribution, temperature of surfaces and masses, dynamic space heat extraction rates, and the cumulative amount of thermal energy extracted by each system. We did not assess the electrical performance for either system; our investigation focused on fundamental thermodynamic differences between radiant cooling and all-air cooling, regardless of the primary cooling sources and mechanical system elements that either may employ.

2.1. Experimental facility

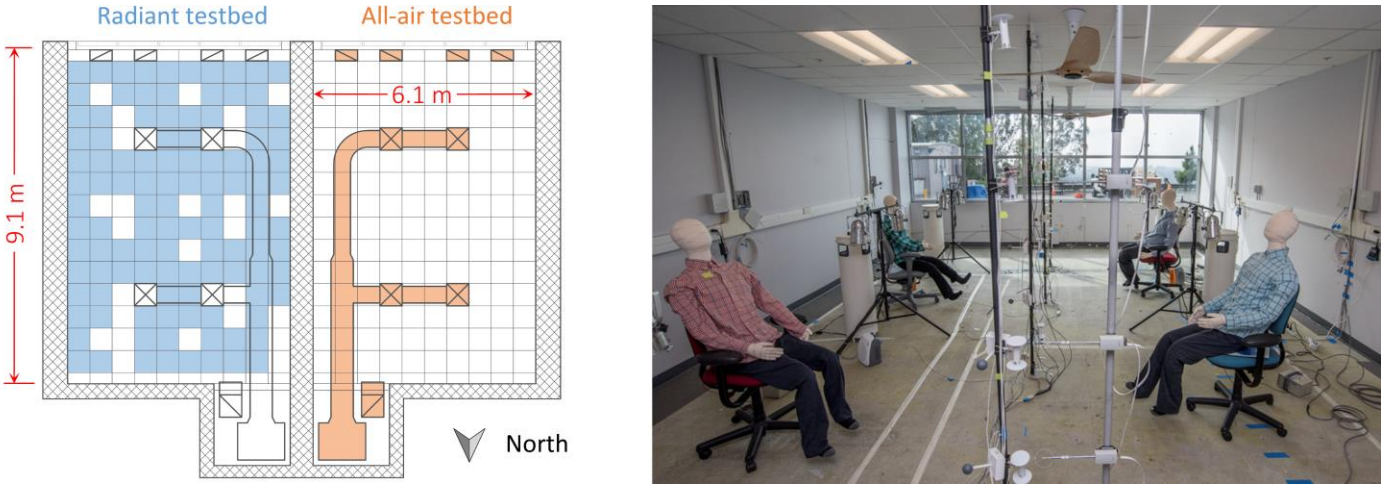

Figure 2: Plan view of testbed buildings (left), and photo of experimental setup (right). Air handler, overhead ductwork, supply diffusers, and return registers in the all-air testbed are highlighted in orange. Low thermal mass metal ceiling panels in the radiant testbed are highlighted in blue.

The experimental facility consisted of two side-by-side testbed buildings, illustrated in Figure 2. Each testbed had 57.6 m^2 (620 ft^2) floor area (6.1 m (20 ft) by 9.1 m (30 ft) interior dimensions, excluding the equipment room) and a 3.66 m (12 ft) high ceiling, with a drop ceiling at 2.74 m (9 ft). The floor was a 15.25 cm (0.5 ft) thick concrete slab with no additional floor covering. The southern wall conformed to ASHRAE 90.1-2010 (ASHRAE 90.1), with 30% window-to-wall ratio and no exterior shading. All other walls, the ceiling, and the floor were very well insulated (U≤0.017 W/m^2-K); in this way each testbed

approximated a single perimeter zone in a larger office building, where the majority of the zone boundary is adjacent to other similarly conditioned zones.

Both testbeds included an independent air handler with overhead supply air distribution and drop-ceiling return plenum. The air handlers were in equipment rooms within the thermal boundary of each testbed. In the radiant cooling testbed the air handler circulated air at a constant 135 m^3/hr (80 cfm), a flow rate representative of typical ventilation rates in radiant buildings (ASHRAE 62.1, Paliaga 2017). The circulated air in the radiant testbed was not conditioned. We chose to include air circulation in the radiant testbed to mimic the air movement characteristics that could be expected in a real building with neutral temperature ventilation air flow. In the all-air testbed the air handler circulated air at a constant flow rate of 1000 m^3/hr (590 cfm) and a proportional integral control sequence adjusted supply air temperature to control the operative temperature. Neither testbed had ventilation air, and the infiltration rate in both testbeds was very small. Tracer gas decay tests indicated infiltration rates of 0.169 and 0.329 air changes per hour in the all-air and radiant testbeds respectively.

The radiant testbed was cooled by a low thermal mass metal ceiling panel system in the drop ceiling (Twa model MOD-RP1). The panels covered 73% of the floor area, as highlighted in blue in Figure 2. We covered as much of the ceiling area as possible to ensure even surface temperature distribution, and to reduce the surface temperature that would be required to extract heat from the testbed. We arranged the panels in six parallel loops with of 19-20 panels in each. Water flowed through the ceiling constantly at 18.2 l/min (4.8 gal/min) and automated controls adjusted the supply water temperature to control the operative temperature in the space. For the experiment with constant internal gains, the median supply water temperature was 16.4 °C with an interquartile range of 3.2 °C. We were careful to ensure that supply water temperature would not cause condensation. The median temperature rise across each loop was 2.2 °C with an interquartile range of 1 °C. Although a low mass radiant system has a distinctly different response time than a high thermal mass radiant system, the heat transfer rate for a surface is determined by the difference between the surface temperature and space air and surface temperatures. Consequently, the observations presented in this article should represent the surface temperatures and surface heat transfer rates that are required for any type of radiant system – including high thermal mass radiant systems – to achieve the indoor conditions observed. However, we do not address the ways that hydronic heat extraction rates would be different for high thermal mass radiant systems.

In the all-air testbed we used a constant volume variable temperature control scheme to provide cooling. We used this strategy instead of a variable-air-volume control scheme so that we could precisely balance heat gain from the fan in the all-air testbed with equivalent heat gain in the radiant testbed.

We supplied internal heat gains to each testbed equally. We used a combination of different electric resistance heating apparatuses that were specially designed and selected to split the amount of convective and radiant heat transfer similar to real heat gains. We measured and balanced all internal heat gains located within the thermal boundary of each testbed, including electricity use for fans, pumps, controls, and data acquisition equipment.

We controlled both testbeds to maintain equal operative temperature setpoints. Although buildings are not regularly controlled to operative temperature, doing so for this comparison ensured equivalent comfort conditions in both testbeds (ASHRAE 55). We believe it is most appropriate to compare radiant and all-air systems with equivalent comfort conditions and not with equivalent air temperatures. The controlled value in each system was the average of three operative temperature measurements, located along the centerline of each testbed, far enough from the south wall to avoid direct solar radiation (3.45 m, 5.3 m and 7.16 m from the south wall), and at 0.6 m height – according to ASHRAE 55 for a seated occupant. We measured

operative temperature with fast response thermistors placed at the center of grey table tennis balls, in accordance with findings from Simone et al. (Simone 2007).

2.2. Measurements and Uncertainty

We monitored more than 250 points in each testbed to assess thermodynamic states and heat transfer rates. We measured these points continuously throughout each experiment and recorded one-minute-average values on one-minute intervals. In summary, categories of measurements included:

- Wall indoor surface temperatures
- Wall internal temperatures
- Slab indoor surface temperatures
- Slab internal temperatures
- Ceiling indoor surface temperatures
- Indoor air temperatures
- Indoor operative temperatures
- Hydronic system temperatures
- Hydronic system water flow rates
- Air system temperatures
- Air system airflow rates
- Internal heat gain rates
- Solar heat gain rates
- Surface heat flux rates
- System controlled variables

Table 1 summarizes the uncertainty for key measurements and calculated metrics. The uncertainty values reported for temperature do not represent the absolute accuracy compared to a standard reference measurement; instead, they describe the calibrated repeatability among the group of measurements compared. Absolute uncertainty is important when values need to be compared to measurements from a separate study, in which case agreement with standard reference measurements is the only way to ensure accurate comparison. Since our experiments compared two cases side-by-side, we were able to calibrate all of our temperature sensors to one another in situ. Since our conclusions focus squarely on whether the space heat extraction rate for the radiant testbed was different from the space heat extraction rate for the all-air testbed, absolute uncertainty compared to a standard reference measurement is not especially relevant, while uncertainty of the difference is very important.

We conducted the in-situ calibration by placing all temperature sensors in a water bath to compare them against one another. The water bath used US Sensor Corp. USP 3021 as reference (uncertainty ±0.01°C to standard reference measurement). We repeated the water bath comparison across a range of temperatures (18 steps between 0-70 °C). Then, we corrected the bias between sensors by adjusting the Steinhart-Hart coefficients for each sensor. This approach nearly eliminates bias between the sensors, consequently uncertainty of the difference between temperature measurements was reduced mainly to stochastic variation in repeated measurements.

Water flow rate measurements were factory calibrated to a standard reference measurement for a wide range of flow rates.

We calculated the sensible space heat extraction rates reported in this article from flow and temperature measurements in the chilled-water loops that served each testbed separately. Flow and temperature measurements were located at the point where chilled water circulating in the cooling plant loop was injected into the loop that serves terminal heat transfer devices. These measurements were located at the thermal boundary of each testbed, and therefore capture all of the thermal energy extracted from each testbed. Since the radiant system was a low thermal mass metal panel ceiling with a fast response time, the hydronic heat extraction rate closely approximates the instantaneous space heat extraction rate associated with convective and radiant heat transfer at the actively cooled ceiling surface. We used propagation of error calculations to determine the uncertainty of the space heat extraction rate for each testbed, and to determine the uncertainty of the difference in heat extraction rate between the two testbeds.

Table 1: Calibrated uncertainty of measurements and calculated metrics

Measurement	Calibrated Uncertainty	Manufacturer and model
Water temperatures	± 0.02 °C	BAPI BA/10K
Air temperatures	± 0.02 °C	US Sensor Corp. PR103J2
Surface temperatures	± 0.02 °C	US Sensor Corp. PR103J2
Water flow rates	± 0.2% of measurement	Siemens MAG 6000 with MAG FM 1100
Internal heat gain rates (electric power)	± 1% of measurement	
Hydronic/space heat extraction rate	± <10 W	Calculated metric

In parallel to propagation of error calculations, we also calibrated the testbeds to one another to improve our confidence in observing any difference between their space heat extraction rates. Prior to the experiments presented here, we conducted two baseline calibrations in which we operated both testbeds as identical all-air systems with constant internal gains for several days. Ultimately, these baseline calibrations yielded a difference in the daily average space heat extraction rates of 1 W – smaller than the magnitude of the uncertainty of the difference due to propagation of uncertainty from the associated measurements.

2.3. Design of Experiments

We conducted two side-by-side experiments, one with constant internal gains, and one with periodic internal gains. We operated each experiment continuously for five days. In all cases the setpoint for operative temperature in the space was 26 °C.

The median value for internal heat gains in each testbed was 3,210 W (55.7 W/m^2 floor area), and ranged from 3,100–3,325 W as grid voltage varied. Heat gains in both chambers varied together, and the median difference between heat gain in each chamber was only 0.85 W. In the first experiment the internal heat gains were constant. In the second experiment we turned on the internal heat gains each day at 06:00 then off at 18:00. Internal gains during the off periods in the second experiment were approximately 400 W (6.9 W/m^2) due to controls and fan energy. Solar gains reached 1,000–1,500 W each day. Meteorological conditions during the experiments were mild, median outdoor temperature was 12.2 °C with interquartile range of 4.75 °C. Consequently, envelope heat transfer was relatively small, and flowed in both directions throughout each day; envelope heat transfer ranged from 15 W/m^2 gains–10 W/m^2 losses. Overall, envelope losses were more dominant than gains. Consequently, the cumulative thermal energy extracted by each system was much smaller than the cumulative thermal energy from internal and solar gains.

For reference, Figure 7 illustrates the solar and internal heat gain cycles for each experiment.

3. RESULTS

3.1. Air, Operative, Surface and Mass Temperatures

In Figures 3–6 we present a detailed comparison of temperature conditions in each testbed during the experiment with constant internal gains. Each figure presents violin plot distributions for temperature measurements at various locations throughout the entire five-day experiment. In addition to each distribution, the plots indicate median values and include whiskers to indicate the interquartile range.

3.1.1. Air temperature distribution

Figure 3 plots the air temperature distribution in each testbed. These measurements demonstrate that air temperature in the all-air testbed was cooler in almost every location. The median differences at each location were as much as 1.5 °C; the average of the median differences was 0.5 °C. Paired by observation time, the Wilcoxon signed rank test indicates a statistically significant difference at all but one location. Paired by location and by observation time, air temperature in the all-air testbed was cooler than the corresponding air temperature in the radiant testbed for 87% of instances ($p < 0.001$).

Among the four horizontal positions, air temperatures nearest the south wall were most different between the two testbeds, and cooler in the all-air testbed – the average of the median differences was 0.88 °C. In the all-air testbed the air temperatures at this horizontal location were also significantly lower than all other locations in the all-air testbed. We suspect that this was related to imperfect air distribution relative to the location of heat gains. All return registers were in the drop ceiling at the south wall (for reference see Figure 2), so the lower temperatures nearer the south wall suggest that some cooled air bypassed the heat gains as the bulk flow moved toward the return. This type of imperfect air distribution is common for all-air systems that use mixing air distribution. The specific pattern is sensitive to the relative locations of heat gains, control points, supply diffusers and return registers. One consequence is that comfort conditions and thermal energy use for the all-air system may be somewhat skewed compared to building energy simulations which typically assume perfect mixing within a zone.

Neither testbed developed strong temperature stratification, although there was some vertical temperature variation in each testbed. Generally, air temperature increased with height, but never by more than 1.5 °C over the 2.5 m range observed. There was a clear tendency for air temperature to decrease near the ceiling in the radiant testbed, while air temperature in the all-air testbed was usually warmest near the ceiling. This inversion is expected with actively cooled ceiling surfaces as natural convection draws cooler air downward from the ceiling surface and draws warmer air upward from heat gains. Other differences in the vertical temperature variation between the two testbeds might be related to the system type, but the differences are within a range that could be attributed to minor locational differences in heat gain, air distribution, or sensor position. For example, we suspect that the reversed inversion pattern at 3.5 m horizontal location in the all-air testbed may have occurred because supply air was not as well mixed at these sensor locations.

These results reinforce the general understanding that air temperature is warmer in radiant cooled buildings than in all-air cooled buildings at equivalent comfort conditions. Therefore, as others have asserted, radiant cooling can reduce heat gain from warm ventilation air compared to an all-air system (Nui 1995, Rhee 2015, Kim 2015-A, Kim 2015-B, Rhee 2017). For the same reason radiant cooling also increases the benefit of cooling from ventilation air when the outside temperature is cooler than indoors.

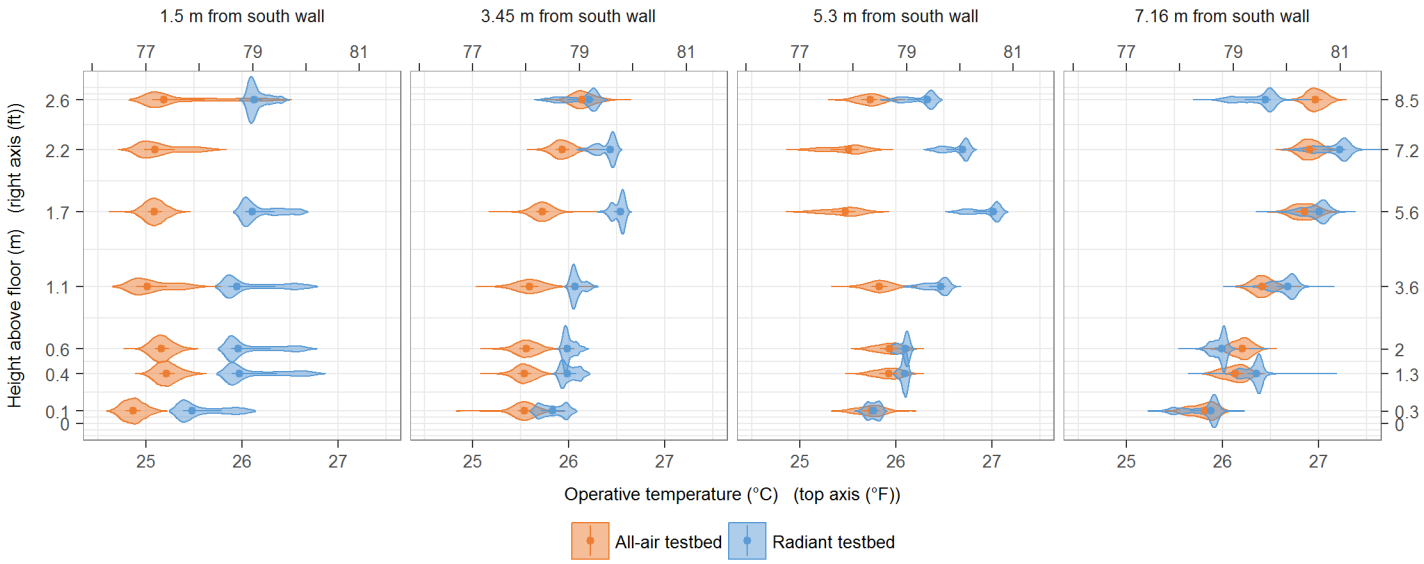

Figure 3: Distribution of air temperatures in each testbed. We measured air temperatures with radiation-shielded thermistors located on a 28-point grid that spanned the south-to-north centerline of each testbed with four horizontal positions and seven vertical positions. Air temperatures in the radiant testbed were warmer in almost every location. The median difference in air temperature was as much as 1.5 °C warmer in the radiant testbed – the average of the median differences was 0.5 °C. The figure plots the distribution of observations at each location, the point in each distribution indicates the median, and the whiskers extending from the median indicate the interquartile range.

3.1.3. Operative Temperature Distribution

We controlled both testbeds to maintain equal operative temperature measured as the average of three sensors at 0.6 m height at three horizontal positions (3.45 m, 5.3 m, and 7.16 m from the south wall). Figure 4 illustrates that operative temperature at the control points was essentially equal in both testbeds – the average of the three median deviations was less than 0.001 °C, which is one order of magnitude less than the sensor uncertainty (± 0.02 °C). However, operative temperatures at other locations were somewhat different from the control points, and there were differences between the two testbeds. In particular, above 1.1 m and nearer the south wall operative temperature was lower in the all-air testbed. The largest median difference between operative temperature at the control points and operative temperature elsewhere was 0.73 °C. The largest median difference between corresponding positions in the two testbeds was 1 °C. These differences were caused mainly by corresponding differences in air temperature. The variation in operative temperature throughout a room is a realistic consequence of nonuniform distribution of heat gains and uneven distribution of cooling. To some extent radiant cooling may be more resilient to non-uniform distribution of heat gains because heat exchange potential is spread out across large areas, and because the space heat extraction rate for an actively cooled surface is somewhat self-regulating – the local surface heat transfer rate naturally adjusts to local heat gains.

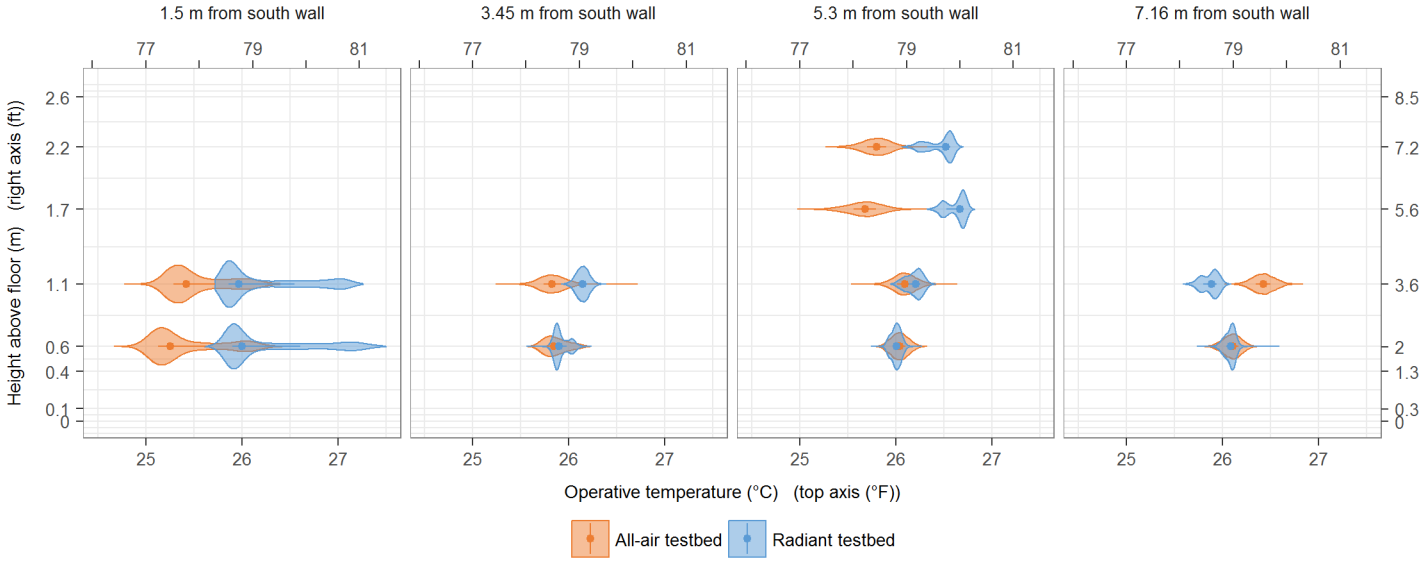

Figure 4: Distribution of operative temperature in each testbed. We measured operative temperature with thermistors placed at the center 40mm diameter plastic spheres, located at various heights and four horizontal positions along the south-to-north centerline of each testbed. The average of the median differences at each of the three control points (0.6 m height and 3.45, 5.3 and 7.16 m from the south wall) was less than 0.001 °C. The differences in operative temperature at other points is attributed mainly to corresponding differences in air temperature. The figure plots the distribution of observations at each location, the point in each distribution indicates the median, and the whiskers extending from the median indicate the interquartile range.

3.1.4. Surface and Mass Temperatures

Figure 5 and Figure 6 compare the temperature of surfaces and masses in each testbed. Figure 5 compares the distribution of temperature measurements from numerous locations, while Figure 6 compares infrared images of each testbed. Each of the distributions in Figure 5 aggregate measurements from between 3–15 thermistors distributed across the surfaces indicated. In every case temperatures of surfaces and masses in the radiant testbed were cooler than in the all-air testbed. Note that in the radiant testbed the indoor surface temperatures were typically cooler than the operative temperature setpoint, while in the all-air testbed the indoor surface temperatures were typically warmer than the setpoint. This occurred because in addition to removing heat directly from internal heat gains by radiant heat transfer, an actively cooled surface also removes heat from all indoor surfaces and masses to which it is exposed. The infrared images in Figure 6 clearly visualize this phenomenon.

Paired by observation time the Wilcoxon signed rank test indicates that each indoor surface in the radiant testbed was cooler than the corresponding surface in the all-air testbed for 100% of instances (p<0.001). The median temperature differences between corresponding indoor wall surfaces in each testbed were between 0.8–1.77 °C (minimum difference = 0.47 °C, maximum difference = 2.22 °C). The median temperature difference between the indoor floor surfaces was 1.85 °C (minimum difference = 1.34 °C, maximum difference = 2.38 °C).

There are two consequences of these surface and mass temperature differences. First, radiant cooled buildings store less heat in non-active masses than all-air buildings. Second, although indoor air temperatures are warmer in radiant buildings, indoor surface temperatures are lower; which increases net gain by heat transfer through the envelope. The change in envelope heat transfer will be small for very well insulated, internal gain dominated buildings, but will be more substantial for buildings with large envelope to floor area ratios, large window to wall ratios, or poorly insulated walls and windows.

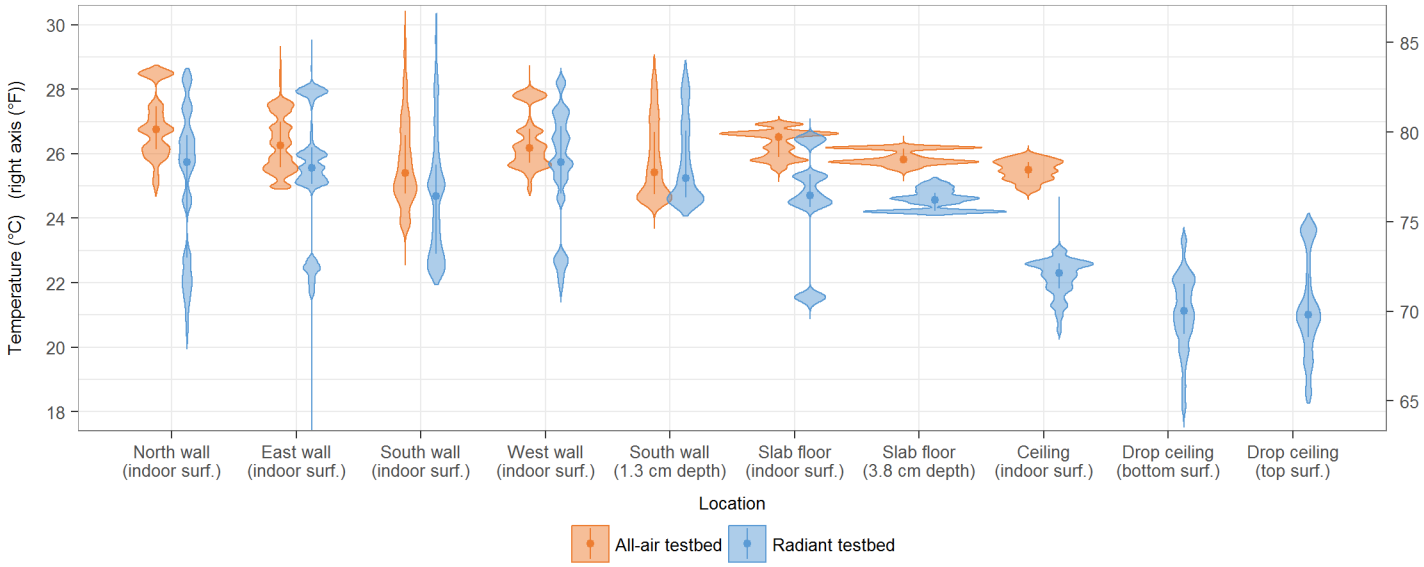

Figure 5:Distribution of surface and mass temperatures in each testbed. We measured surface temperatures with low mass thermistors taped to surfaces. Sensors for "South Wall (1.3 cm depth)" were located between the wallbaord and insulation. Sensors for "Slab Floor (3.8 cm depth)" were located in the middle of each concrete slab. Sensors for "Drop ceiling (bottom suf.)" were located on the bottom surface of the actively cooled low thermal mass metal panel radiant ceiling, at the center of the first and last panels in each of 6 parallel loops. The low thermal mass metal panel radiant ceiling included 1" fiberglass insulation with radiation shielding; sensors for "Drop ceiling (top surf.)" were located on top of the insulation. Paired by observation time, indoor surfaces in the radiant testbed were cooler than corresponding surfaces in the all-air testbed for 100% of instances. The figure plots the

distribution of observations at each location, the point in each distribution indicates the median, and the whiskers extending from the median indicate the interquartile range.

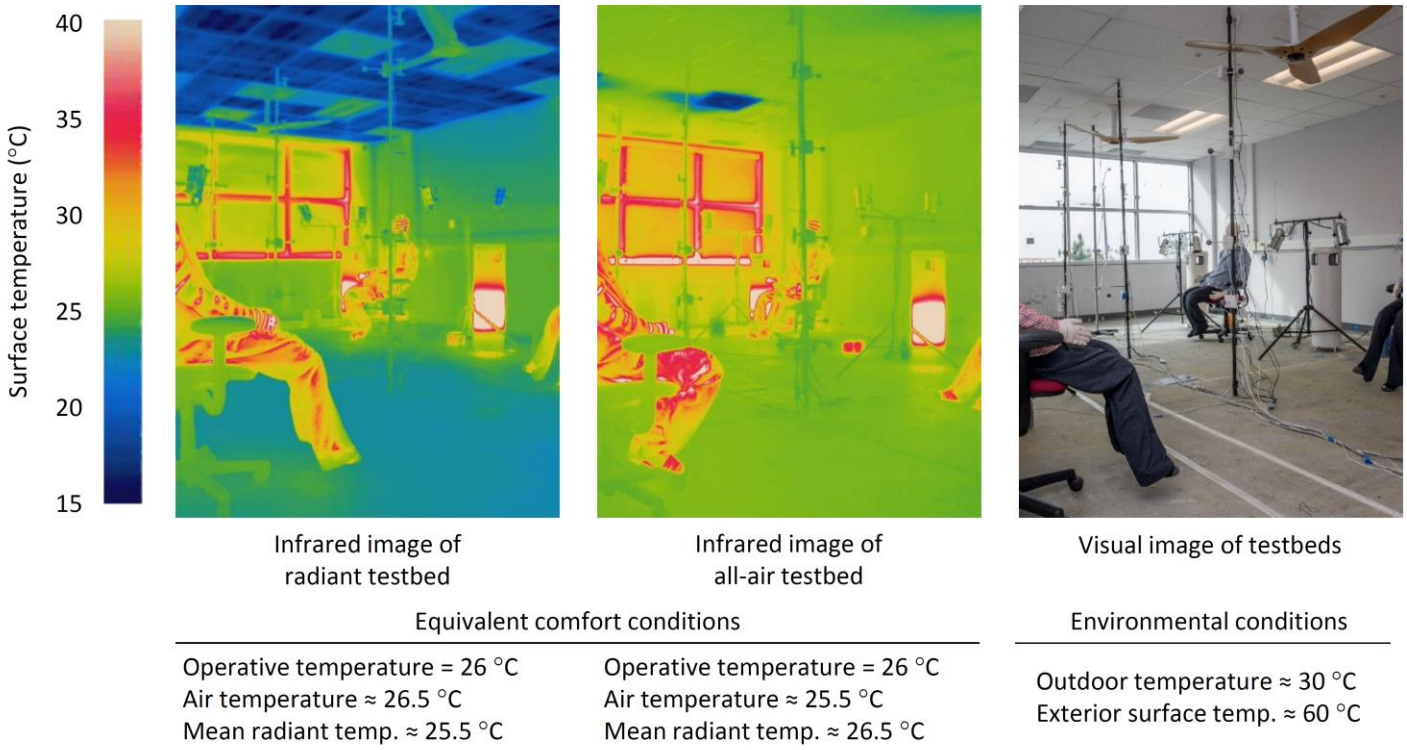

Figure 6: Infrared images of radiant testbed (left) and all-air testbeds (center) while cooling, with equal internal gains and equal solar gains, during experiment with constant internal gains. At the time of the infrared images (11:00–13:00 on 7 Sept. 2016), temperature of outdoor air was ~30°C, and temperature of the exterior cladding on the south wall was ~60°C. Although comfort (operative temperature) was equivalent in both testbeds, all surfaces and masses in the radiant testbed were cooler, which indicates that less heat was stored in the non-active masses of the radiant testbed.

3.2. Cooling Rates and Thermal Energy

Figures 7–9 compare the dynamic thermal response for each testbed in both experiments. Each figure shows results for the experiment with constant internal heat gains on the left, and results for the experiment with periodic internal heat gains on the right. The observations reveal fundamental differences between radiant and all-air systems.

3.2.1. Operative Temperature Response

Figure 7 compares the operative temperature response in each testbed for the two experiments. A more detailed view of two days for the experiment with periodic internal heat gains is included in the Appendix. For both experiments, each system type maintained operative temperature at 26 °C during all periods that required cooling. In the experiment with constant internal heat gains both cooling systems operated continuously. In the experiment with periodic internal heat gains both cooling systems turned off while the internal gains were at a reduced level because the operative temperature naturally remained lower than the setpoint.

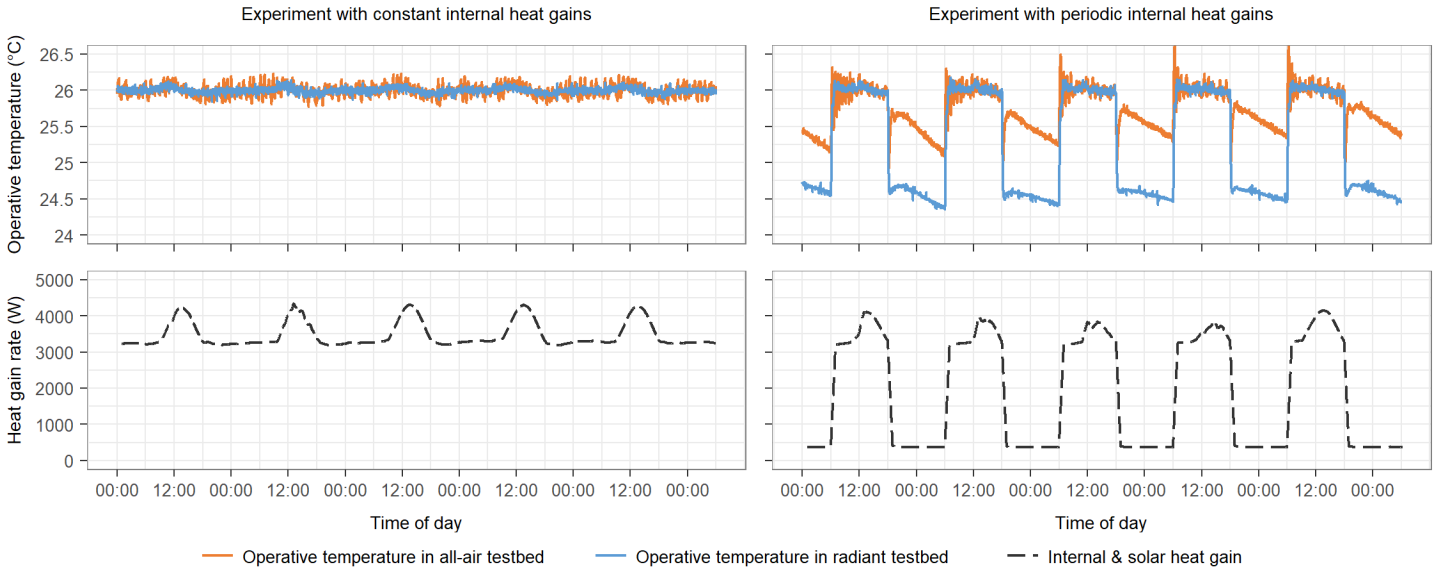

Figure 7: Operative temperature (top row) and combined internal and solar heat gain rate (bottom row) for experiment with constant internal gains (left) and experiment with periodic internal gains (right). The figure plots operative temperature at one-minute intervals, and heat gain rate as one-hour rolling averages at one-minute intervals.

In the experiment with periodic internal heat gains, operative temperatures in both testbeds decreased rapidly for 10–15 minutes after the internal gains were removed. Air temperatures – which are not shown in Figure 7 – also decreased at a similar rate. This temperature decrease was due to the thermal inertia of chilled-water and cooling equipment that remained after the internal gains were removed.

After the initial decline, operative temperatures and air temperatures in the all-air testbed increased for 1–2 hr because heat that had been absorbed in the building mass during the day was released into the space by convection to the air and radiation to the other surfaces. The operative temperatures and air temperatures returned to within 0.25 °C of the values from immediately before the heat gains were removed. Afterward, over the course of the night, operative temperature and air temperature declined steadily as heat stored in the building mass was rejected passively to the environment.

The corresponding operative temperature response for the radiant testbed was distinctly different. After the initial rapid decline, operative temperatures and air temperatures did not increase as they did in the all-air

testbed. Since radiant buildings store less heat in masses, they release less heat into the room from masses after internal and solar gains diminish. Concomitantly, buildings with radiant cooling also reject less heat to the environment by passive means. A portion of the heat that would be absorbed by masses in an all-air building during the day then lost to the environment overnight is instead extracted by the radiant system earlier in the day. We expect that this pattern would be most pronounced in climates with large diurnal temperature variation, and especially in scenarios where natural ventilation is used overnight to precool the building mass. It would be less pronounced in scenarios with fewer opportunities for passive heat rejection. Furthermore, we expect that the control strategy – such as whether or not precooling or night setback are employed – will also influence the extent to which each system type enables passive heat rejection to the environment.

3.2.2. Dynamic space heat extraction rates

Figure 8 compares the dynamic space heat extraction rate generated by each system in the two experiments. A more detailed view of two days for the experiment with periodic internal gains is included in the Appendix. For both systems, we calculated the space heat extraction rate from flow and temperature measurements in the chilled-water loop serving each testbed. Since the radiant system was a low thermal mass metal panel ceiling with a fast response time, this measurement closely approximates the instantaneous space heat extraction rate associated with convective and radiant heat transfer at the actively cooled ceiling surfaces.

The results reveal that to maintain comfort conditions equivalent to an all-air system:

1. Radiant cooling must extract heat from gains earlier
2. The peak space heat extraction rate must be larger for radiant systems
3. The peak space heat extraction must occur earlier for radiant systems

These differences arise in response to dynamic heat gains, and would not occur at steady state in an adiabatic system. To maintain consistent comfort conditions as heat gains increase, radiant cooling must extract heat earlier than an all-air system because a portion of the increasing heat gain that would be absorbed by masses in an all-air building is instead removed by radiant heat transfer to the actively cooled surfaces.

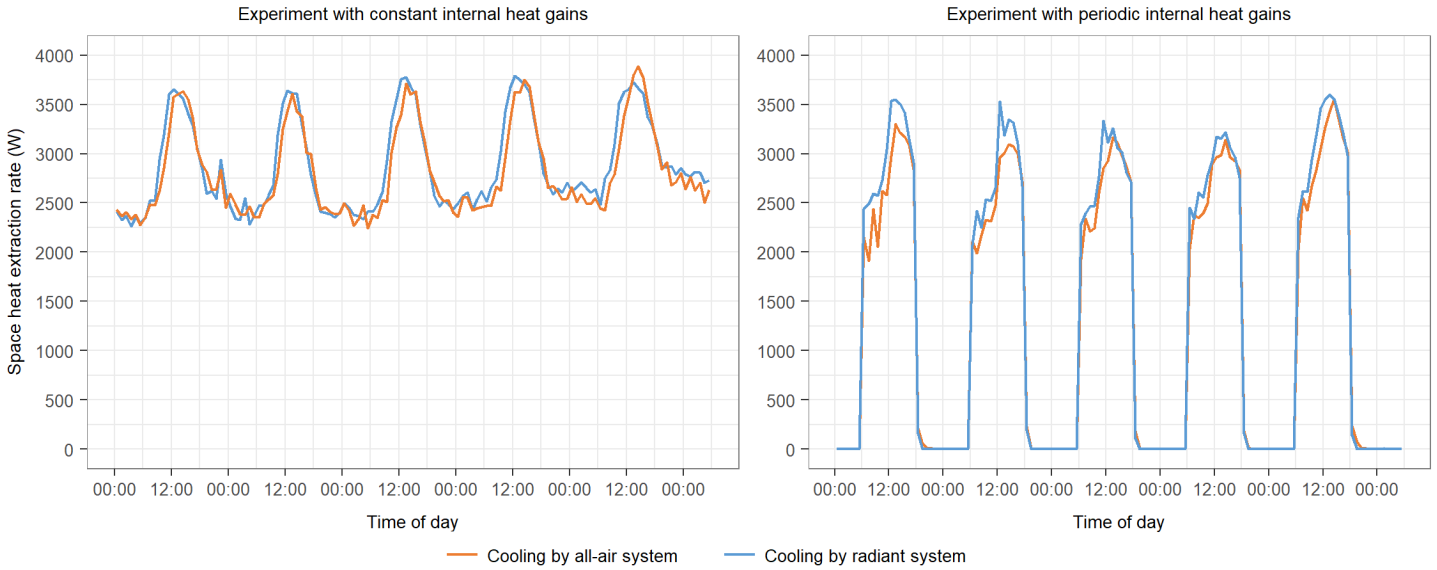

Figure 8: Space heat extraction rates for radiant (blue) and all-air systems (orange) in experiment with constant internal heat gains (left) and experiment with periodic internal heat gains (right). Data is plotted as one-hour rolling averages at one-hour intervals.

In the experiment with constant internal heat gains the differences in space heat extraction rate were driven by changes in solar gain each day. Except for the last day of the experiment, the peak space heat extraction rate in the radiant testbed was 1–3% larger (0.7–1.6 W/m^2) and occurred 1–2 hr earlier. In the experiment with periodic internal heat gains the peak space heat extraction rate in the radiant testbed was 2–10% larger (1.3–5.6 W/m^2) and occurred 1–2 hr earlier.

These results confirm that to maintain equivalent operative temperature the peak sensible space heat extraction rate for a radiant system must be larger than the peak sensible space heat extraction rate for an all-air system. This finding has consequences for the design of radiant systems; in particular, as Feng et al. indicated (Feng 2013), industry common practice methods for design sizing of the terminal cooling devices for all-air systems will underestimate the peak space heat extraction rates required for radiant systems.

The scenarios presented here represent cases with realistic solar and internal gains, but they do not represent every reasonable possibility. The magnitude of the difference in space heat extraction rate will be smaller in some circumstances and larger in others. The magnitude of the difference will depend on:

1. The amplitude of the daily oscillation in heat gain
2. The ratio of radiant heat gains to convective heat gains
3. The thermal diffusivity and volume to surface area ratio of masses within and enclosing the space

We expect that the difference will be larger when the amplitude of the daily oscillation in heat gain is larger, and smaller when it is smaller. For example, in a hypothetical scenario with an adiabatic envelope and constant internal heat gains the steady state space heat extraction rate would be equal for both system types.

We expect that the difference would be larger in scenarios with mainly radiant heat gains and smaller for scenarios with mainly convective heat gains. For example, in a hypothetical scenario where oscillating heat gains are composed entirely of shortwave radiation, the space heat extraction required for the all-air system would be limited to the heat that is shed by convection from non-active masses that have absorbed the heat gains. Whereas radiant cooling would extract a portion of the shortwave gains directly, and would rapidly extract heat absorbed by the non-active masses by way of longwave radiant heat transfer.

Lastly, we expect that the difference would be larger in scenarios where the temperature of surfaces within and enclosing a space are more resilient to heat gain – where exposed surfaces have high thermal diffusivity and high thermal capacity. These high thermal mass surfaces, such as exposed concrete construction, are readily available to absorb heat from the radiant component of heat gains without a substantial increase in surface temperature. Low thermal mass surfaces such as raised floors, drop ceilings, or furniture would tend to decrease the difference between the dynamic heat extraction rates for radiant and all-air systems. These low thermal mass surfaces more rapidly convert radiant heat gains to convective heat gains.

3.2.3. Cumulative thermal energy use

Lastly, Figure 9 plots the cumulative thermal energy extracted by each system over the course of the two experiments. The results reveal that to maintain equivalent comfort radiant cooling must remove somewhat more heat from a building than all-air cooling. The difference is small but meaningful. In the experiment with constant internal heat gains radiant cooling extracted 2% more heat overall; and for the experiment with periodic internal heat gains radiant cooling extracted 7% more heat overall. These differences equate to an average difference in the space heat extraction rate of 60 W (1 W/m^2) and 183 W (3.2 W/m^2) respectively. For context, the uncertainty in the difference between space heat extraction rates for the two testbeds was approximately 15 W at the conditions observed – an order of magnitude lower than the observed difference.

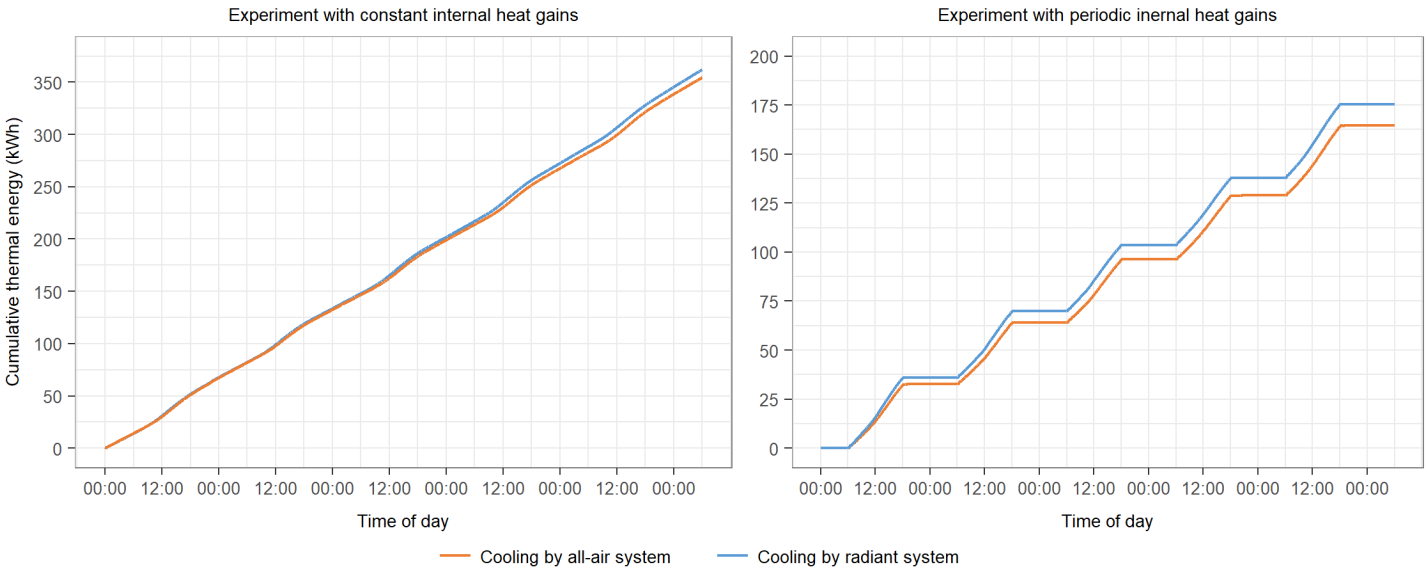

Figure 9: Cumulative space heat extraction energy for radiant (blue) and all-air systems (orange) in experiment with constant internal heat gains (left) and experiment with periodic internal heat gains (right). Data plotted on one-minute intervals.

These results reinforce the findings associated with Figure 7. Whereas the differences in the dynamic space heat extraction would exist even in an adiabatic system, the additional cumulative thermal burden for radiant cooling exists specifically because of interactions with the environment. The difference in the cumulative space heat extraction energy can be attributed to two factors:

1. Buildings with radiant cooling have lower interior surface temperatures which increases envelope heat gains.
2. Buildings with radiant cooling store less heat in non-active masses and subsequently reject less heat to the environment by passive means.

4. DISCUSSION

We have experimentally confirmed, far beyond the bounds of measurement uncertainty, that the dynamic space heat extraction rate for radiant cooling is different from the dynamic space heat extraction rate for all-air cooling when both systems maintain equal operative temperature. The differences observed in our experiments are generally similar to differences indicated by previous simulations and simplified laboratory experiments (Feng 2013, Feng 2014) – and therefore provide conclusive evidence that these differences are present in realistic circumstances.

However, we expect that the magnitude and characteristics of the difference depend on many variables including: the type of heat gains, the magnitude of heat gains, the timing of heat gains, the location of heat gains, the physical and thermal characteristics of non-active masses, the sizing and layout of actively cooled surfaces, the outdoor conditions, and control of the cooling system.

Despite these many influences, the general phenomenological differences observed in our experiments should extend to other scenarios where radiant cooling and all-air cooling are compared at equivalent operative temperatures. For example, if operative temperature in both testbeds followed a dynamic profile throughout the day – as typically occurs in buildings with high thermal mass radiant systems – space heat extraction rates would be somewhat different from what we observed, but the peak space heat extraction rate would still be larger for the radiant system and it would occur earlier.

We assessed thermal energy extracted from the space, and we did not assess the way that high thermal mass radiant systems decouple the space heat extraction rate from operation of the cooling plant. For a high thermal mass radiant system, the space heat extraction rate is different from the hydronic heat extraction rate – see Figure 1 for further clarification. Although our results have confirmed that the peak space heat extraction rate for radiant surfaces must be larger than the peak space heat extraction rate for an all-air system, we also acknowledge that a strategically controlled high thermal mass radiant system could allow the cooling plant to be much smaller than what would be required for an all-air system in equivalent circumstances.

Although industry common practice methods for design sizing of terminal cooling devices do not properly capture the differences between radiant and all-air systems, researchers have developed building energy simulation tools that do account for the differences properly (Feng 2013, Feng 2014). Many buildings with radiant cooling operate successfully every day despite the shortcoming of common design methods. This may be because designers for radiant buildings use building energy simulation tools that account for the differences, or it may be because designers employ a factor of safety in practice that is large enough to overcome the differences.

Finally, while our results have confirmed that radiant cooling must remove more heat than an all-air system in order to maintain equivalent comfort conditions, we also acknowledge that radiant cooling enables several efficiency opportunities that can result in overall primary energy savings compared to all-air cooling. Many building energy simulation studies have clearly established that properly designed radiant cooling systems can achieve substantial primary energy savings and peak electrical demand reduction compared to conventional all-air cooling systems.

Furthermore, although we have focused exclusively on cooling, similar differences should also exist between radiant and all-air systems in heating mode – the peak space heating rate would be larger for radiant heating systems, and more heat would be required each day.

5. CONCLUSIONS

Niu et al. (1995) and Feng et al. (2013,2014) previously indicated that the dynamic space heat extraction rates for radiant cooling and all-air cooling are different. However, industry common practices used for design sizing of terminal cooling devices do not recognize these differences. We conducted a series of laboratory tests to substantiate or refute the claimed differences. Whereas the previous studies were based on simulations and a simplified environmental chamber experiment, we conducted a series of experiments in much more realistic circumstances. We used a pair of equivalent side-by-side testbed buildings that enabled thorough assessment of building energy systems at a realistic physical scale, with naturally occurring solar gains, and natural interaction with the surrounding environment. For each experiment we operated the two testbeds simultaneously, imposed equivalent internal gains, and controlled each system to maintain equivalent operative temperatures.

We conclude that radiant cooling and all-air cooling remove heat from buildings in different ways. The experiments presented herein demonstrate that these differences influence the dynamic space heat extraction rates that are required to maintain equal comfort conditions in response to dynamic heat gains. We corroborate the previous claims by Niu et al (1995) and Feng et al (2013, 2014): the time and rate at which heat must be extracted from a space depend on the type of terminal device used for cooling. To maintain comfort conditions equivalent to an all-air system: (1) radiant cooling must extract heat from gains earlier; (2) the peak space heat extraction rate must be larger for radiant systems; and (3) the peak space heat extraction must occur earlier for radiant systems.

The differences are mainly due to the way that heat gains are absorbed by, stored in, and released from non-active masses. Radiant cooling extracts heat from all surfaces in a building, so when internal or solar gains increase, a portion of the heat that would be absorbed by mass in an all-air building is extracted by the radiant surface instead. As a result, all interior surfaces in a radiant building are cooler than in an equivalent all-air building, and less heat is stored in mass. In our experiments non-active interior surfaces were as much as 2.38 °C cooler in the radiant testbed, and air temperatures were as much as 1.75 °C warmer.

These differences increase the cumulative amount of heat that must be extracted each day. Although the indoor air temperature is warmer in a radiant building, net gains by envelope heat transfer are larger than an all-air building because the interior surfaces of exterior walls are cooler. More importantly, since less heat is stored in non-active masses, radiant buildings reject less heat to the environment by passive means. As a result, in our experiments, despite having equal internal and solar gains, the cumulative amount of heat extracted from the radiant testbed was as much as 7% larger than the all-air testbed.

Finally, to maintain equivalent comfort conditions, the dynamic space heat extraction rate for radiant cooling must be different from that of all-air cooling. In our experiments, the peak space heat extraction rate was as much as 10% larger in the radiant testbed, and it occurred 1–2 hours earlier. These findings are of consequence for: the design and sizing of radiant surfaces, the choice and sizing of hydronic systems and cooling plants, the dynamic control of these systems, and the resulting potential for electricity savings and demand response. It is especially important to note that the peak sensible space heat extraction rate for radiant cooling – the heat transfer rate at the surface – must be larger than that of an all-air system in an equivalent building with equivalent operative temperature conditions. These findings should be true for all radiant system types, regardless of their thermal mass.

6. ACKNOWLEDGMENTS

This work was supported by the California Energy Commission (CEC) Electric Program Investment Charge (EPIC) (EPC-14-009) “Optimizing Radiant Systems for Energy Efficiency and Comfort” and the Center for the Built Environment at University of California Berkeley. The research would not have been possible without the considerable efforts from many individuals at Lawrence Berkeley National Laboratory and UC Berkeley Center for the Built Environment, nor without the input and guidance from numerous industry partners and academic collaborators. We are particularly grateful to Ari Harding, Darryl Dickerhoff, Cindy Regnier, Baisong Ning, Eleftherios Bourdakis, and Gwelen Paliaga for their exceptional contributions.

7. DECALARATION OF INTERESTS

The Center for the Built Environment at the University of California Berkeley – with which the authors are affiliated, is advised by and funded in part by many partners that represent a diversity of organizations from the building industry – including manufacturers, building owners, facility managers, contractors, architects, engineers, government agencies, and utilities.

8. REFERENCES

ANSI/ASHRAE/IENSA Standard 90.1-2010 Energy Standard for Buildings Except Low-Rise Residential Buildings, American Society of Heating, Refrigerating and Air-Conditioning Engineers, Inc., 2010.

ANSI/ASHRAE 62.1-2013 - Ventilation for Acceptable Indoor Air Quality, American Society of Heating, Refrigerating and Air-Conditioning Engineers, Inc., 2013.

J. (Dove) Feng, F. Bauman, S. Schiavon, Critical review of water based radiant cooling system design methods, in: Proceedings of Indoor Air 2014, International Society of Indoor Air Quality and Climate, Hong Kong, 2014. http://escholarship.org/uc/item/2s00x6ns.

J. (Dove) Feng, F. Bauman, S. Schiavon, Experimental comparison of zone cooling load between radiant and air systems, Energy and Buildings. 84 (2014) 152–159. doi:10.1016/j.enbuild.2014.07.080.

J. (Dove) Feng, S. Schiavon, F. Bauman, Cooling load differences between radiant and air systems, Energy and Buildings. 65 (2013) 310–321. doi:10.1016/j.enbuild.2013.06.009.

H.E. Feustel, C. Stetiu, Hydronic radiant cooling – preliminary assessment, Energy and Buildings. 22 (1995) 193–205. doi:10.1016/0378-7788(95)00922-K.

X. Hao, G. Zhang, Y. Chen, S. Zou, D.J. Moschandreas, A combined system of chilled ceiling, displacement ventilation and desiccant dehumidification, Building and Environment. 42 (2007) 3298–3308. doi:10.1016/j.buildenv.2006.08.020.

C. Higgins, 2016 list of zero net energy buildings, (2016). https://newbuildings.org/wp-content/uploads/2016/10/GTZ_2016_List.pdf (accessed December 1, 2017).

C. Higgins, K. Carbonnier, Energy performance of commercial buildings with radiant heating and cooling, (2017). http://escholarship.org/uc/item/34f0h35q.

J.-W. Jeong, S.A. Mumma, W.P. Bahnfleth, Energy conservation benefits of a dedicated outdoor air system with parallel sensible cooling by ceiling radiant panels, in: ASHRAE Transactions, American Society of Heating Refrigerating and Air-Conditioning Engineers, 2003 Annual Meeting, Kansas City, Missouri, 2003: volume 100, part 2, pp. 627–636.

K.W. Kim, B.W. Olesen, Part one: radiant heating and cooling systems, ASHRAE Journal. 57 2 (2015) 28–37.

K.W. Kim, B.W. Olesen, Part two: radiant heating and cooling systems, ASHRAE Journal. 57 3 (2015) 39–42.

B. Lehmann, V. Dorer, M. Koschenz, Application range of thermally activated building systems, Energy and Buildings. 39 (2007) 593–598. doi:10.1016/j.enbuild.2006.09.009.

I. Maor, S. Snyder, Evaluation of factors impacting EUI from high performance building case studies, High Performance Buildings. Fall (2016) 30–38. http://www.hpbmagazine-digital.org/hpbmagazine/fall_2016?pg=32#pg32 (accessed December 1, 2017).

T. Moore, Potential and limitations for hydronic radiant slabs using waterside free cooling and dedicated outside air systems, in: Proceedings of Third National Conference of IBPSA-USA, International Building Performance Simulation Association, Berkeley, California, 2008: pp. 148–155.

New Buildings Institute, Getting to zero 2012 status update: a first look at the costs and features of zero energy commercial buildings, (2012). https://newbuildings.org/wp-content/uploads/2015/11/GettingtoZeroReport_01.pdf (accessed December 1 2017).

J. Niu, J. v.d. Kooi, H. v.d. Rhee, Cooling load dynamics of rooms with cooled ceilings, Building Services Engineering Research and Technology. 18 4 (1997) 201–207. doi:10.1177/014362449701800404.

J. Niu, J. v.d. Kooi, H. v.d. Rhee, Energy saving possibilities with cooled-ceiling systems, Energy and Buildings. 23 (1995) 147–158. doi:10.1016/0378-7788(95)00937-X.

J.L. Niu, L.Z. Zhang, H.G. Zuo, Energy savings potential of chilled-ceiling combined with desiccant cooling in hot and humid climates, Energy and Buildings. 34 (2002) 487–495. doi:10.1016/S0378-7788(01)00132-3.

G. Paliaga, M. Dawe, M. Goebes, P. Eilert, Integrated packages for advanced buildings towards ZNE, in: Proceedings of ACEEE Summer Study on Energy Efficiency in Buildings, American Council for an Energy-Efficient Economy, Asilomar, CA, 2016. http://aceee.org/files/proceedings/2016/data/papers/3_636.pdf (accessed October 13, 2017).

G. Paliaga, F. Farahmand, P. Raftery, J. Woolley, TABS Radiant Cooling Design & Control in North America: Results from Expert Interviews, UC Berkeley, Center for the Built Environment (2017). http://escholarship.org/uc/item/0w62k5pq.

K.-N. Rhee, K.W. Kim, A 50 year review of basic and applied research in radiant heating and cooling systems for the built environment, Building and Environment. 91 (2015) 166–190. doi:10.1016/j.buildenv.2015.03.040.

K.-N. Rhee, B.W. Olesen, K.W. Kim, Ten questions about radiant heating and cooling systems, Building and Environment. 112 (2017) 367–381. doi:10.1016/j.buildenv.2016.11.030.

D.O. Rijksen, C.J. Wisse, A.W.M. van Schijndel, Reducing peak requirements for cooling by using thermally activated building systems, Energy and Buildings. 42 (2010) 298–304. doi:10.1016/j.enbuild.2009.09.007.

A. Simone, J. Babiak, M. Bullo, G. Landkilde, B. Olesen, Operative temperature control of radiant surface heating and cooling systems, in: Proceedings of Clima 2007 Wellbeing Indoors, REHVA World Congress, Helsinki, Finland, 2007. http://www.irbnet.de/daten/iconda/CIB8368.pdf (accessed December 1, 2017).

F. Sodec, Economic viability of cooling ceiling systems, Energy and Buildings. 30 (1999) 195–201. doi:10.1016/S0378-7788(98)00087-5.

C. Stetiu, Radiant cooling in US office buildings: Towards eliminating the perception of climate-imposed barriers, PhD Dissertation, University of California, Berkeley, 1998. doi:10.2172/650256.

C. Stetiu, Energy and peak power savings potential of radiant cooling systems in US commercial buildings, Energy and Buildings. 30 (1999) 127–138. doi:10.1016/S0378-7788(98)00080-2.

R.K. Strand, K.T. Baumgartner, Modeling radiant heating and cooling systems: integration with a whole-building simulation program, Energy and Buildings. 37 (2005) 389–397. doi:10.1016/j.enbuild.2004.07.009.

R.K. Strand, C.O. Pedersen, Modeling radiant systems in an integrated heat balance based energy simulation program, ASHRAE Transactions, American Society of Heating Refrigerating and Air-Conditioning Engineers, 2002 Annual Meeting, Honolulu, Hawaii, 2002: Vol. 108, Pt. 2. pp. 979.

Z. Tian, J.A. Love, Energy performance optimization of radiant slab cooling using building simulation and field measurements, Energy and Buildings. 41 (2009) 320–330. doi:10.1016/j.enbuild.2008.10.002.

Z. Tian, J.A. Love, Application of radiant cooling in different climates: assessment of office buildings through simulation, in: Proceedings of Eleventh International IBPSA Conference, International Building Performance Simulation Association, Glasgow, Scotland, 2009: pp. 2220–2227. http://www.ibpsa.org/proceedings/BS2009/BS09_2220_2227.pdf (accessed December 1, 2017).

T. Yu, P. Heiselberg, B. Lei, M. Pomianowski, Validation and modification of modeling thermally activated building systems (TABS) using EnergyPlus, Building Simulation. 7 (2014) 615–627. doi:10.1007/s12273-014-0183-6.

10. APPENDIX

10.1. Dynamic space heat extraction rates and operative temperature response

For clarity, Figure 10 repeats the data presented in Figures 7–8 for the first two days from the experiment with periodic internal heat gains. The operative temperature responses illustrate that buildings with radiant cooling store less heat in non-active masses, and so reject less heat to the environment by passive means. The space heat extraction rates illustrate that to maintain comfort conditions equivalent to an all-air system: (1) radiant cooling must extract heat from gains earlier; (2) the peak space heat extraction rate must be larger for radiant systems; and (3) the peak space heat extraction must occur earlier for radiant systems. The difference in space heat extraction rates also reveal that radiant cooling must extract more heat over the course of each day.

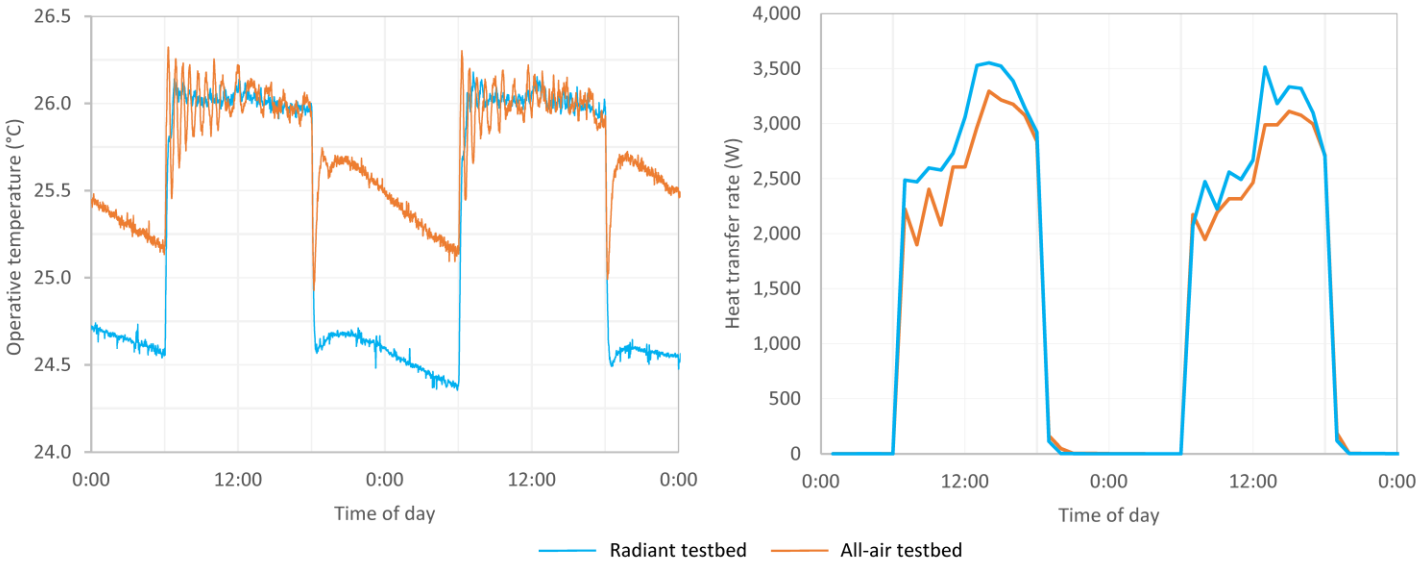

Figure 10: Operative temperature response (left) and space heat extraction rates (right) for the radiant testbed (blue) and the all-air testbed (orange) for the first two days from the experiment with periodic heat gains.). The figure plots operative temperature at one-minute intervals, and space cooling rate as one-hour rolling averages at one-hour intervals.

10.2. Operative temperature and air velocity in each testbed

Human thermal comfort is influenced by several indoor environmental parameters including air temperature, mean radiant temperature, and air motion. Operative temperature is a concept that captures the combined effects of heat transfer by convection and radiation between a human occupant and a non-uniform thermal environment. The metric is used by all standards for thermal comfort in indoor environments as the best single predictor for comfort (ISO EN 7730, EN 15251, AleftSHRAE 55).

Since radiant cooling exchanges heat with occupants differently than all-air cooling, it is imperative that performance of the two systems be compared at equivalent comfort conditions, not at equivalent air temperature. For this reason we averaged the measurement of operative temperature at three locations in each testbed and controlled both systems to an operative temperature set point of 26 °C.

Operative temperature is a calculated parameter that depends on measurement of globe temperature, air temperature, and air velocity:

$$T_O = \frac{(\bar{T}_R \cdot h_R + T_A \cdot h_C)}{(h_C + h_R)}$$

where T_O is the operative temperature, T_A is the air temperature, $\bar{T}_R$ is the mean radiant temperature, h_C is the convective heat exchange coefficient for a person, and h_R is the radiant heat exchange coefficient for a person.

For environments with low air velocity, the convective heat transfer coefficient and radiant heat transfer coefficient are similar, so the operative temperature can be approximated as the average of the mean radiant temperature and the air temperature (ISO EN 7730, EN 15251, ASHRAE 55). In a study that compared various apparatus for measuring operative temperature at low air velocity Simone et al showed that measuring temperature at the center of a small grey colored sphere approximates operative temperature to within 0.2 C, as long as the sensor is not located too close to a wall.

We used hot wire anemometers to measure air velocity in both testbeds to ensure that it was low enough to comply with the aforementioned assumptions about operative temperature. Figure 11 illustrates the results. The distributions represent velocity measurements at each position over a ten-minute period during steady operation. Air velocity was acceptably low throughout both testbeds.

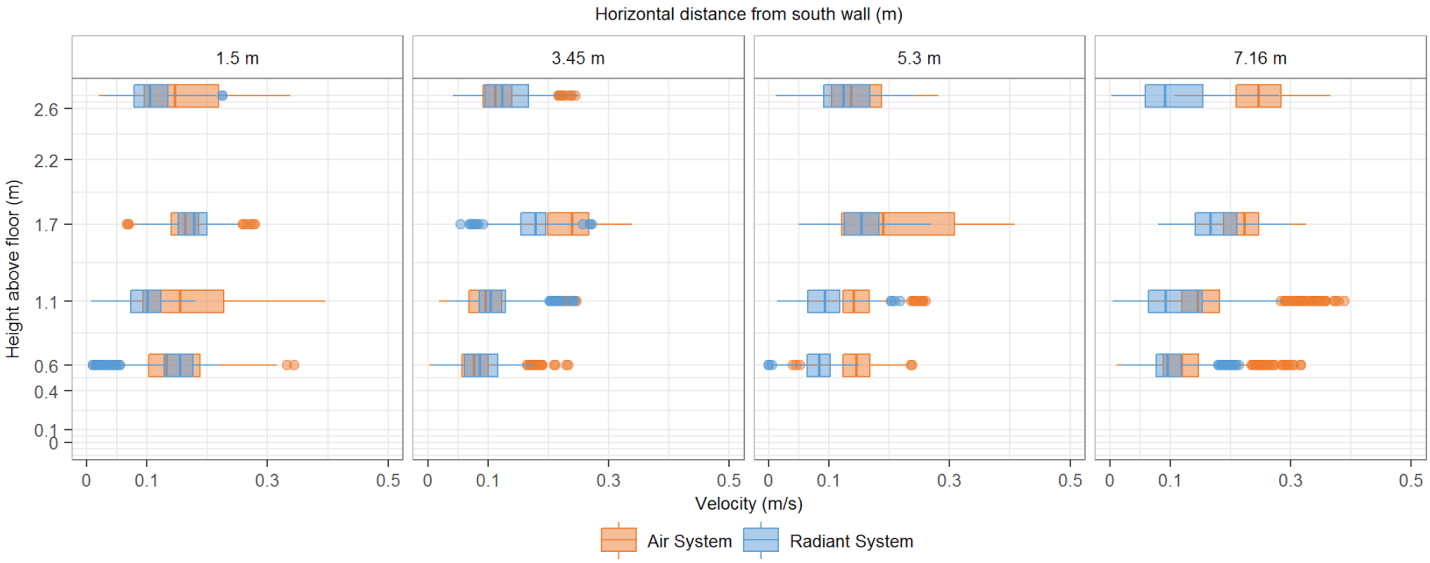

Figure 11: Distribution of air speed in each testbed. The comparisons presented in this paper were conducted with both testbeds at equivalent comfort conditions. Air speed measurements indicate that air speed was similar in both testbeds, and low enough that it would not appreciably influence the measurement of operative temperature.